















Novel engineered nanobodies specific for N-terminal region of alpha-synuclein recognize Lewy-body pathology and inhibit *in-vitro* seeded aggregation and toxicity

Issam Hmila¹ , Nishant N. Vaikath¹ , Nour K. Majbour¹ , Daniel Erskine² , Indulekha P. Sudhakaran¹ , Vijay Gupta¹ , Simona S. Ghanem¹ , Zeyaul Islam³ , Mohamed M. Emara^{4,5} , Houari B. Abdesselem¹ , Prasanna R. Kolatkar³ , Devaya K. Achappa⁶ , Tatiana Vinardell^{6,7}  and Omar M. A. El-Agnaf¹ 

1 Neurological Disorder Research Center, Qatar Biomedical Research Institute (QBRI), Hamad Bin Khalifa University (HBKU), Qatar Foundation, Doha, Qatar

2 Translational and Clinical Research Institute, Newcastle University, UK

3 Diabetes Center, Qatar Biomedical Research Institute (QBRI), Hamad Bin Khalifa University (HBKU), Qatar Foundation, Doha, Qatar

4 Basic Medical Sciences Department, College of Medicine, QU Health, Qatar University, Doha, Qatar

5 Biomedical and Pharmaceutical Research Unit, QU Health, Qatar University, Doha, Qatar

6 Equine Veterinary Medical Center, Qatar Foundation, Doha, Qatar

7 College of Health & Life Science, Hamad Bin Khalifa University, Qatar Foundation, Doha, Qatar

Keywords

aggregated alpha-synuclein; Lewy body; nanobody; Parkinson's disease

Correspondence

O. M. A. El-Agnaf, Qatar Biomedical Research Institute, Hamad Bin Khalifa University, P.O. Box 34110, Doha, Qatar
Tel: +97455935568
E-mail: oelagnaf@hbku.edu.qa

(Received 11 May 2021, revised 28 September 2021, accepted 26 January 2022)

doi:10.1111/febs.16376

Nanobodies (Nbs), the single-domain antigen-binding fragments of dromedary heavy-chain antibodies (HCAb), are excellent candidates as therapeutic and diagnostic tools in synucleinopathies because of their small size, solubility and stability. Here, we constructed an immune nanobody library specific to the monomeric form of alpha-synuclein (α -syn). Phage display screening of the library allowed the identification of a nanobody, Nb α -syn01, specific for α -syn. Unlike previously developed nanobodies, Nb α -syn01 recognized the N-terminal region which is critical for *in vitro* and *in vivo* aggregation and contains many point mutations involved in early PD cases. The affinity of the monovalent Nb α -syn01 and the engineered bivalent format BivNb α -syn01 measured by isothermal titration calorimetry revealed unexpected results where Nb α -syn01 and its bivalent format recognized preferentially α -syn fibrils compared to the monomeric form. Nb α -syn01 and BivNb α -syn01 were also able to inhibit α -syn-seeded aggregation *in vitro* and reduced α -syn-seeded aggregation and toxicity in cells showing their potential to reduce α -syn pathology. Moreover, both nanobody formats were able to recognize Lewy-body pathology in human post-mortem brain tissue from PD and DLB cases. Additionally, we present evidence through structural docking that Nb α -syn01 binds the N-terminal region of the α -syn aggregated form. Overall, these results highlight the potential of Nb α -syn01 and BivNb α -syn01 in developing into a diagnostic or a therapeutic tool for PD and related disorders.

Abbreviations

A β , Abeta; BBB, blood-brain barrier; CD, circular dichroism; DLB, dementia with Lewy bodies; HCAb, heavy-chain antibody; HNE, hydroxynonenal; ITC, isothermal titration calorimetry; LB, Lewy bodies; mAb, mouse monoclonal antibody; MSA, multiple system atrophy; NAC, non-amyloid component; Nb, nanobody; PD, Parkinson's disease; scFvs, single-chain antibody fragments; α -syn, alpha-synuclein.

Introduction

The aggregation of the protein alpha-synuclein (α -syn) is linked to the onset and progression of a range of neurodegenerative disorders including Parkinson's disease (PD), dementia with Lewy bodies (DLB) and multiple system atrophy (MSA) collectively known as α -synucleinopathies [1–4]. PD and DLB are characterized by the intraneuronal accumulation of misfolded α -syn into Lewy bodies (LB) and Lewy neurites (LN), whereas the key pathological hallmark of MSA is the presence of glial cytoplasmic inclusion (GCI) in oligodendrocytes. α -Syn is a 140-amino acid long protein that is abundant in the presynaptic terminal. The amino acid sequence of α -syn can be divided into three regions with distinctive characteristics. The N-terminal segment (1–60) of α -syn is positively charged and regulates interactions with lipid-membrane regions and contains six imperfectly conserved repeats (KTKEGV) that may facilitate protein-protein binding. This N-terminal segment was also reported to contain point mutations that lead to early-onset autosomal dominant Parkinsonism [5–10]. The non-amyloid component (NAC) central segment (61–95) of α -syn is hydrophobic and is critical for initial aggregation [11]. The negatively charged C-terminal region (96–140) is involved in the aggregation process [12].

Owing to its central role in PD pathogenesis, α -syn has been the main target for therapeutic approaches against synucleinopathies. Multiple therapeutic strategies have been opted to target α -syn including stabilizing its physiological conformation, decreasing its expression, inhibiting its aggregation, increasing intracellular clearance and also transmission-directed approaches that include uptake by neighbouring cells and enhancing extracellular clearance mechanisms [13]. One of the approaches for inhibiting the aggregation of α -syn is the use of antibodies. Many antibodies and antibody fragments have been generated against different regions of α -syn [14]. However, conformation-specific monoclonal antibodies specific for α -syn oligomers/aggregates were shown to be effective in reducing the accumulation of α -syn oligomers in multiple brain regions of transgenic mice overexpressing α -syn [15]. A humanized version of mouse monoclonal antibody (mAb) 9E4 has been tested in a phase 2 clinical trial in 2017 [16]. In addition, a human-derived α -syn antibody generated by screening human memory B-cell libraries from healthy elderly individuals, that binds to α -syn residues 1–10, is currently under investigation in a phase 2 clinical trial for PD [17]. However, a major drawback, to the routine use of monoclonal antibodies for immunotherapeutic uses, is their large size that is

sub-optimal for crossing the blood-brain barrier thereby creating difficulties in administering therapeutic doses from peripheral administration sites. Antibody fragments thus can offer several advantages over the use of conventional antibodies. Their small size allows access to challenging and cryptic epitopes, they have better tissue penetration and have demonstrated reduced immunogenicity. Many single-chain antibody fragments (scFvs) have been selected and characterized against α -syn protein. These scFvs bind to α -syn C-terminal region, NAC region or bind to oligomeric forms of α -syn and inhibit aggregation and toxicity of α -syn *in vitro* [18–22]. However, the functional expression of these scFvs is low and their stability remains questionable.

Nanobodies (Nbs) are the antigen-binding domains derived from heavy-chain only antibody (HCAb), a type of immunoglobulin found in Camelidae family [23]. Since their discovery, Nbs have demonstrated their potential application in various fields of research, biotechnology and medicine. Nbs are highly soluble, very robust and easily amenable to generate multivalent or multispecific constructs with low cost of production. Nbs have high affinity for their target and their small size (15 kDa) make them less immunogenic and enable high tissue penetrability. Recently, a bivalent Nb designed for the treatment of thrombotic thrombocytopenic purpura was approved by FDA [24]. These advantages make Nbs ideal candidates for use in therapeutic or diagnostic approaches for synucleinopathies. Several Nbs raised against monomeric α -syn have been developed: NbSyn2 and NbSyn87 bind to distinct epitopes within the C-terminal region of monomeric α -syn and can recognize its fibrillar forms [25–27] and reduce oligomer-induced cellular toxicity [28]. However, no α -syn Nb is currently being tested in clinical trials for neurological diseases.

In order to further explore the potential of Nbs in synucleinopathies, we generated a VHH library from α -syn immunized dromedary. Subsequent phage display screening, we identified a nanobody, Nb α -syn01 that was found to be specific for α -syn. Pepscan revealed that the epitope recognized by Nb α -syn 01 lies in the N-terminal region of α -syn sequence that was found to contain many point mutations involved in early PD cases. This nanobody was subsequently used to reconstruct into a tandem linked bivalent format, BivNb- α -syn01. The interaction of the monovalent and bivalent nanobody formats with α -syn was evaluated by ITC, CD and slot blot. Both Nb α -syn01 and BivNb α -syn01 were found to have higher affinity for α -syn fibrils than monomeric form and did not cross-react with any other amyloid proteins or other

members of the synuclein family, including β - or γ -synuclein. Furthermore, the two nanobody formats were able to block α -syn aggregation *in vitro* and α -syn aggregates-induced toxicity in cells. The two Nbs formats were also able to detect Lewy-body pathology in human post-mortem brain tissues from PD cases.

Results

Identification of the binding region by epitope mapping

Nanobody library was constructed after immunization of the camel with several injections with monomeric α -syn. Nb-syn01 was identified after four rounds of phage display screening of the nanobody library against monomeric α -syn (Fig. 1A). From the gene of Nb α -syn01, a bivalent format was constructed by linking the two nanobodies by human IgA hinge. The purification of the construct showed pure proteins according to the Coomassie staining of the SDS/PAGE (Fig. 1B). The nanobody yield after purification was $\sim 2 \text{ mg}\cdot\text{L}^{-1}$ of *Escherichia coli* culture for both Nb α -syn01 and BivNb α -syn01. To identify the epitope recognized by Nb α -syn01, we carried out pepscan using overlapping peptide library composed of synthetic 14-mer peptides spanning the entire length of α -syn (Fig. 1C). Nb α -syn01 was found to bind to N-terminal region of α -syn peptide no. 7 corresponding to amino acids 43–56 (Fig. 1C,D). This was further confirmed by checking the binding of Nb α -syn01 with identified peptide along with the adjacent peptides from the library in preabsorption experiment. We found that only peptide 43–56 inhibited the binding of Nb α -syn01 α -syn coated plates confirming the epitope (Fig. 1E). Interestingly, this region is rich in point mutations observed in early-onset PD cases [5–10]. This region is also a part of the pre-NAC region identified previously as an important modulator of α -syn aggregation *in vitro* and *in vivo* [29,30].

Characterization of the binding interactions of Nb α -syn01 with monomeric and fibrillar forms of α -syn by ITC

The binding affinity and thermodynamic parameters of Nb α -syn01 and its bivalent format against monomeric and fibrillar forms of α -syn were investigated using ITC. Unexpectedly, Nb α -syn01 was observed to have higher affinity towards fibrils ($2.44\text{E-}7 \text{ M}$) than to monomeric α -syn ($1.91\text{E-}6 \text{ M}$) (Fig. 2A–D). The bivalent format of the nanobody showed a decrease in dissociation constant (K_d ; improved affinity) for both

α -syn formats with higher affinity to the fibrils ($2.67\text{E-}8 \text{ M}$) compared to monomeric form ($9.43\text{E-}8 \text{ M}$) (Fig. 2E). The data obtained of ΔH , ΔG and $-\Delta S$ for all interactions showed that the interactions are favourable and enthalpically driven (Fig. 2F–I).

Specificity of Nb α -syn01 and its bivalent format to α -syn fibrils

In order to further evaluate the binding interactions and specificity of our nanobody towards α -syn monomers and fibrils, we tested the reactivity of Nb α -syn01 and BivNb α -syn01 with different quantities of monomeric and fibrillar forms of α -syn by blotting using vacuum filtration methods. The result confirms that Nb α -syn01 has higher affinity towards α -syn fibrils than the monomers (Fig. 3A). The bivalent format BivNb α -syn01 showed an increased affinity to both α -syn fibrils and monomers with more selectivity towards fibrils than monomer (Fig. 3A). Next, we tested the reactivity of the two forms of Nbs (Nb α -syn01 or BivNb α -syn01) to different oligomers of α -syn cross-linked by hydroxynonenal (HNE) and dopamine (DA). The crosslinking stabilizes the oligomers and prevents their transition to the thermodynamically favourable fibrillar form. Both Nb α -syn01 and BivNb α -syn01 showed higher reactivity to HNE-oligomers than DA-oligomers (Fig. 3B). The higher reactivity of these Nbs to the HNE- α -syn oligomers might be due to the different unique structures of the oligomers and the epitope can be more exposed in the HNE-oligomers than in DA-oligomers. Furthermore, the specificity of these Nbs was also assessed for their cross-reactivity with other amyloidogenic proteins including Abeta 42 (A β 42), Tau40, and ABri in their monomeric and fibrillar forms. Nb α -syn01 and BivNb α -syn01 showed no cross-reactivity to these amyloid proteins. The monomers and fibrils of these amyloid protein samples showed good reactivity to their respective control antibodies (Fig. 3C).

Interestingly, and unlike other α -syn antibodies that target N-terminal segment of the protein, both Nb α -syn01 and the BivNb α -syn01 did not cross-react with monomers or fibrils of β - and γ -syn (Fig. 3D), showing that they are specific to α -syn. The comparison of the amino acids sequences of the peptide 43–56 of these three proteins showed that β -syn differs by three amino acids (position K45R, H50Q and T54S) and γ -syn differs by four amino acids to α -syn (position G47N, H50Q, G51S and T54S) (Fig. 3E). The amino acids in these positions of α -syn are critical in binding to the Nb. Finally, the specificity of these Nbs was also evaluated against mouse α -syn, and we found that

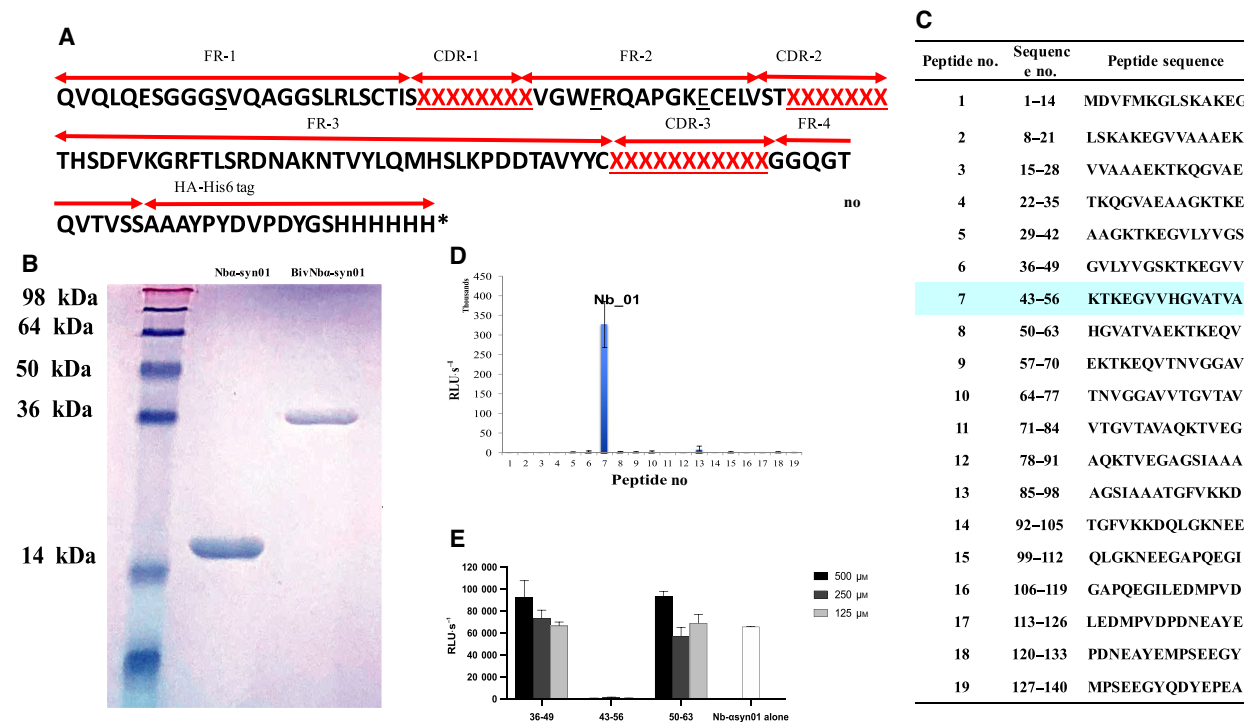


Fig. 1. (A) Amino acids deduced sequence of Nb α -syn01. The VHH-hallmark amino acids are underlined. (B) SDS/PAGE showing the purity of two constructs Nb α -syn01 and bivalent Biv Nb α -syn01 with molecular weight of 15 and 30 kDa respectively. (C) Table describing the sequences of the peptides used for Pepscan. (D) Epitope mapping using α -syn peptide library by ELISA. Bar graph showing the mean and standard deviation (SD) of chemiluminescence signal (RLU·s⁻¹) obtained from duplicate values. Nb α -syn01 showed a strong signal with peptide no. 7 corresponding to amino acid 43–56 of α -syn. (E) Preabsorption experiment of Nb α -syn01 preincubated with 500, 250 or 125 μ M of the peptides. Bar graph shows the mean and SD of chemiluminescence signal (RLU·s⁻¹) obtained from duplicate values.

Nb α -syn01 and BivNb α -syn01 recognized both human and mouse α -syn (Fig. 3D), indicating a common target epitope. The two proteins differ in this region by only one amino acid A53T which did not affect the binding affinity and indicated that Nb binds to the N-terminal region of the peptide.

Secondary structure study of nanobodies with α -syn monomers and fibrils

The secondary structure of the two nanobodies was checked with circular dichroism as individual proteins and in complex with α -syn monomers or fibrils. The monomeric α -syn alone showed a typical spectrum of unfolded protein without any secondary structure (Fig. 4A,B). The individual CD spectra of nanobody and α -syn fibrils showed a profile with high β sheet structure (Fig. 4C,D) as evident from the negative minimum absorption at wavelength \sim 220 nm and a positive maximum at \sim 198 nm. When nanobody was complexed with α -syn monomers, there was no perturbation in the structure (Fig. 4A,B). Same results were

obtained where both Nbs in complex with α -syn fibrils and showed a profile that no perturbation was detected in the secondary structure of fibrils after nanobody binding structure (Fig. 4C,D).

The effect of Nb α -syn01 on *in vitro* induced α -syn seeded fibril formation

We assessed if our Nb α -syn01 could inhibit the seeding-process of α -syn monomers into fibrils using an *in vitro* assay. We incubated α -syn seeds either alone or with Nb α -syn01 or BivNb α -syn01 for 1 h at 37 °C, following which α -syn monomers (25 μ M) were added and incubation was further carried on till 6 h time-point. Nb α -syn01 and BivNb α -syn01 significantly inhibited α -syn monomers seeded-aggregation at concentrations of 8 and 2 μ M respectively with *P*-values = < 0.05 as denoted by the lower Th-S counts (Fig. 5A). The lower concentration of the bivalent BivNb α -syn01 needed for the inhibition might be the result of higher avidity acquired due to its bivalent nature compared to Nb α -syn01. Transmission electron

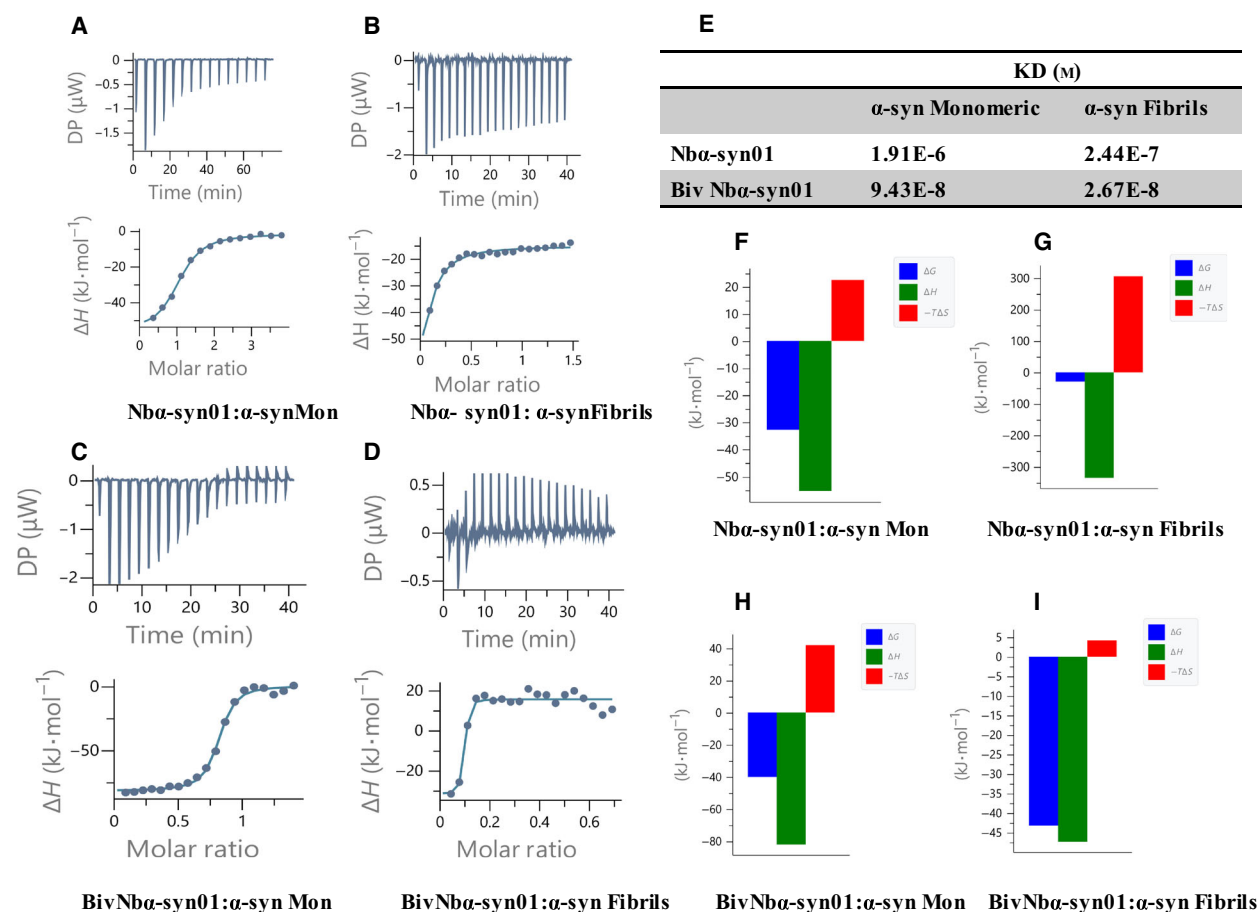


Fig. 2. ITC experiment for the affinity interaction between (A) Nba-syn01: α -synMon, (B) Nba-syn01: α -syn fibrils, (C) BivNba-syn01: α -syn Mon, (D) BivNba-syn01: α -syn Fibrils and (E) KD (M) constant of Nba-syn01 and BivNba-syn01 to monomeric and fibrillar forms of α -syn. (F–I) ΔG , ΔH and $-T\Delta S$ measured for the binding of Nba-syn01 and BivNba-syn01.

microscopy images from the samples further confirmed the efficiency of the Nbs in inhibiting α -syn seed-induced aggregation (Fig. 5B).

The effect of the two nanobody formats on α -syn seeded induced toxicity

The process of amyloid fibrillation causes the formation of oligomeric/fibrillar intermediates thereby leading to cell death [31–33]. To check whether our Nbs have the capacity to affect α -syn-mediated aggregation followed by cellular toxicity, a previously described cell-viability MTT assay was employed [33–35]. In the MTT assay, the tetrazolium salt MTT is converted to formazan with the help of mitochondrial dehydrogenase that utilizes the living cells respiration function. First, we incubated SH-SY5Y cells with α -syn seeds (2 μ M) alone following which α -syn monomers (10 μ M) were added and the seeds promoted aggregation via monomers, thus inducing

cytotoxicity. Earlier published work has shown that α -syn monomers enhanced α -syn seed-dependent toxicity upon addition [33,35]. To perform the MTT assay, α -syn seeds in the presence or absence of Nba-syn01 and BivNba-syn01 were added to SH-SY5Y cells in two identical sets. One set was with α -syn monomer and second set was without monomer addition. As shown in Fig. 6, Nba-syn01 and BivNba-syn01 inhibited α -syn seeds-induced toxicity, resulting in a significantly greater number of viable cells (Fig. 6, P -values = < (0.05 – 0.001)). Nba-syn01 and BivNba-syn01 both decreased α -syn seeds-induced toxicity whether we added monomer or not, showing that both seeded-aggregation and seed-induced toxicity were inhibited. As Nbs co-incubated with α -syn seeds reduced toxicity without concomitant application of monomers, this may be due to blocking the seeding for the endogenous α -syn monomers and that Nbs might reduce internalization of seeds and their related seeded aggregation of α -syn.

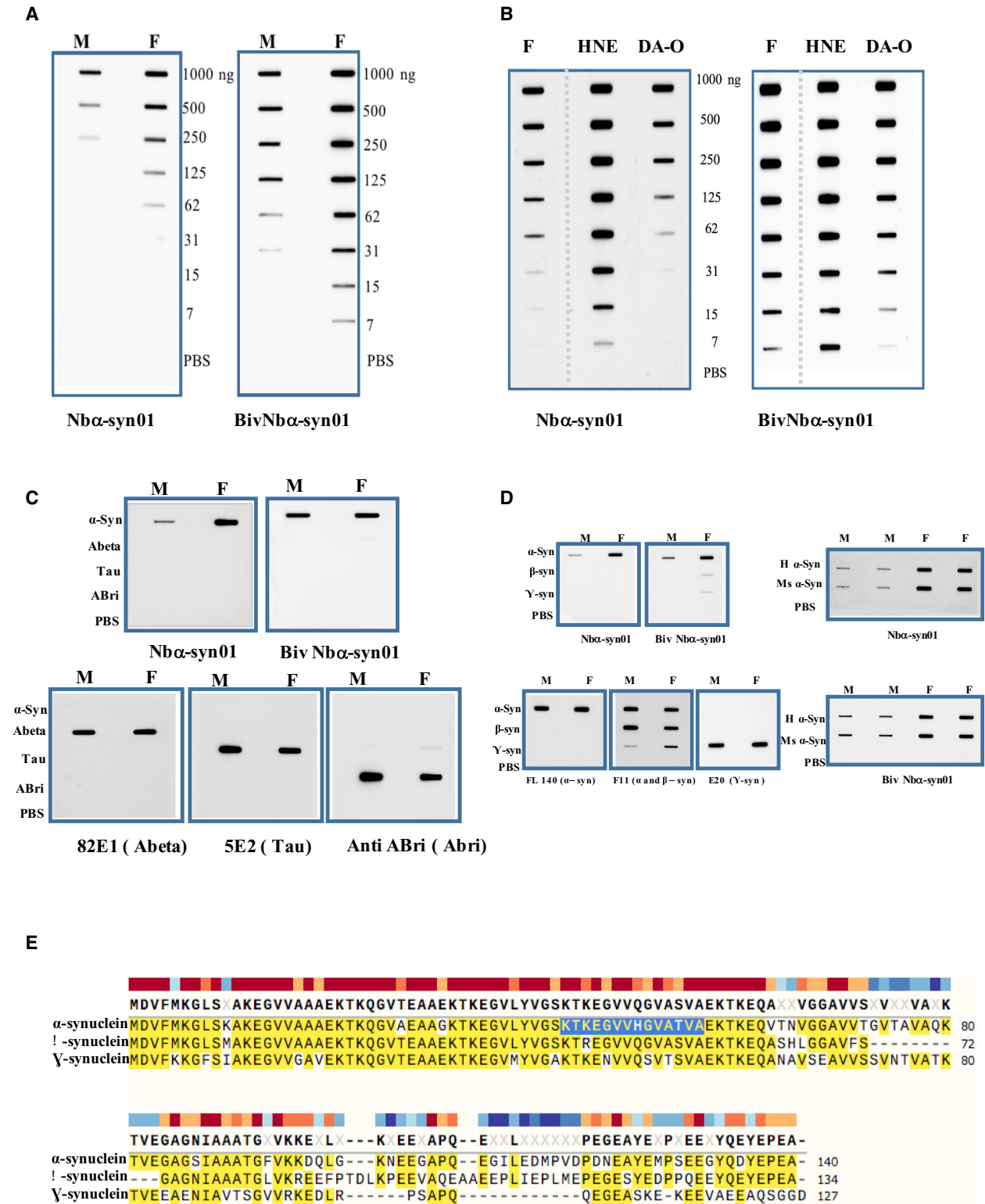


Fig. 3. (A) Blotting results showing reactivity of Nb α -syn01 (left) and BivNb α -syn01 (right) to monomers and fibrils (1 μ g to 7 ng) of full length α -syn (140) are coated on nitrocellulose membrane. (B) The reactivity of Nb α -syn01 (left) and Biv Nb α -syn01 (right) to α -syn (140) fibrils and α -syn oligomers cross-linked by HNE and Dopamine (DA) coated from 1 μ g to 7 ng (C) Blot result showing the reactivity of Nb α -syn01 and Biv Nb α -syn01 to 50ng monomers and fibrils of different amyloid proteins α -syn, Abeta (A β 42), Tau and ABri coated on nitrocellulose membrane. Bottom panel shows α -syn, Abeta (A β 42), Tau and ABri tested with other control mAbs 82E1, 5E2 and Anti-ABri corresponding to Abeta, Tau and ABri respectively. (D left). The reactivity of Nb α -syn01 and BivNb α -syn01 to 50 ng monomers and fibrils of synuclein family of proteins α -syn, β -syn and γ -syn coated on nitrocellulose membrane. Bottom panel shows the α -syn, β -syn and γ -syn samples (50 ng) tested with control antibodies FL140, F11, and E20 antibodies that react with α -syn, α/β syn and γ -syn respectively. (Right) The reactivity of Nb α -syn01 (above) and Biv Nb α -syn01 (below) to 50 ng of recombinant human and mouse α -synuclein (140) monomers and fibrils. (E) Sequence alignment of human α -, β - and γ -synuclein protein sequences. The peptide 43–56 is highlighted in blue. Residues are coloured in yellow to indicate identity across all three synucleins.

Nb α -syn01 and bivalent format detect Lewy bodies in human brain tissues from PD and DLB patients

We investigated if Nb α -syn01 and BivNb α -syn01 can identify PD-associated pathology in human brain *post-mortem* tissue. For the purpose, we utilized formalin-fixed paraffin-embedded samples from patients with neuropathological and clinical symptoms of DLB. Nb α -syn01 and BivNb α -syn01 did not show any immunoreactivity in controls in the DMV (Fig. 7A,C) or in AD in the entorhinal cortex (Fig. 7E,G), implying neither antibody cross-reacts with tau pathology in AD. Interestingly, Nb α -syn01 and BivNb α -syn01 recognized solid granular deposits indicative of Lewy-

body pathology in both the dorsal motor nucleus of the vagal nerve (DMV; Fig. 7B,D) and entorhinal cortex (Fig. 7F,H).

Structure prediction and potential interaction of Nb α -syn01 with α -synuclein

We performed the Nb α -syn01 structure homology modelling using SWISS-MODEL [36]. The SWISS-MODEL template library was searched with BLAST and HHBLITS for evolutionary related structures matching the Nb α -syn01 sequence. Sequence alignment of Nb α -syn01 sequence with top five templates highlights the conservation of amino acid residues and any one of these templates can be used for homology modelling.

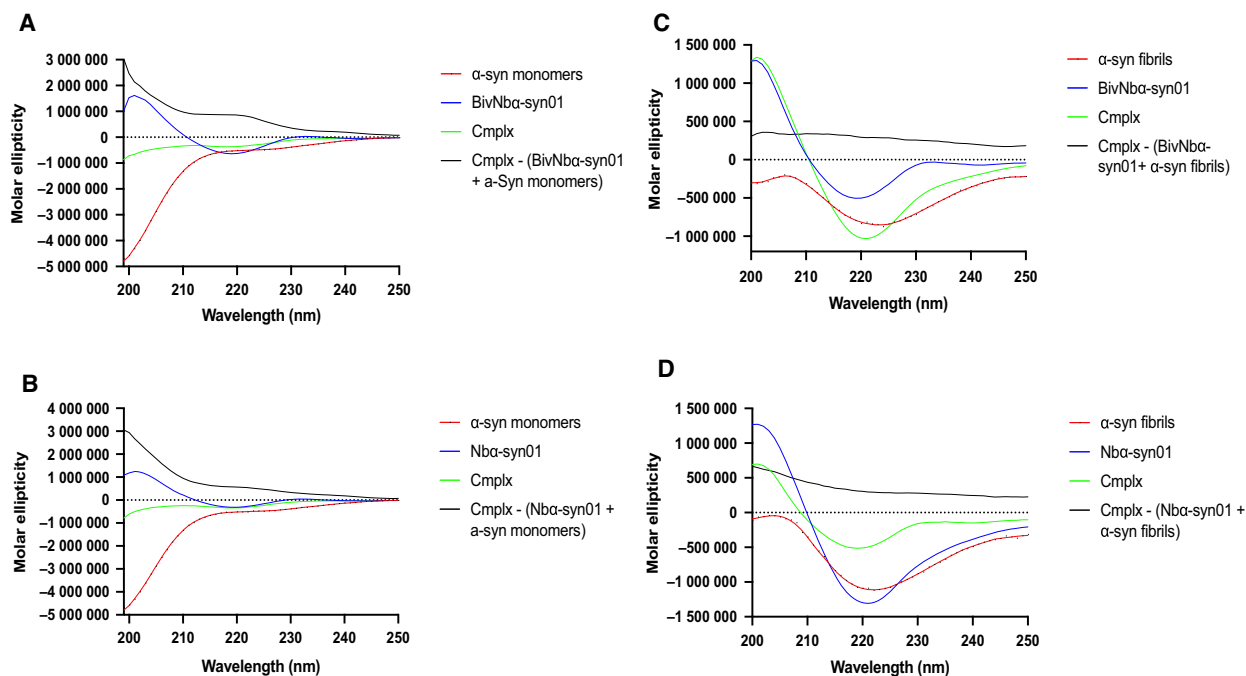


Fig. 4. The interaction of 5 μ M of Nb α -syn01 or BivNb α -syn01 with 5 μ M of α -syn monomeric or α -syn fibrils by CD. CD spectra for Nbs with monomeric form (A, B) or with α -syn fibrils (C, D). The spectrum represents the mixture of Nb construct with the monomeric or fibrils α -syn are in green. The spectrum of the difference Nb: α -syn Fibrils – (Nb + α -syn Fibrils) is in black.

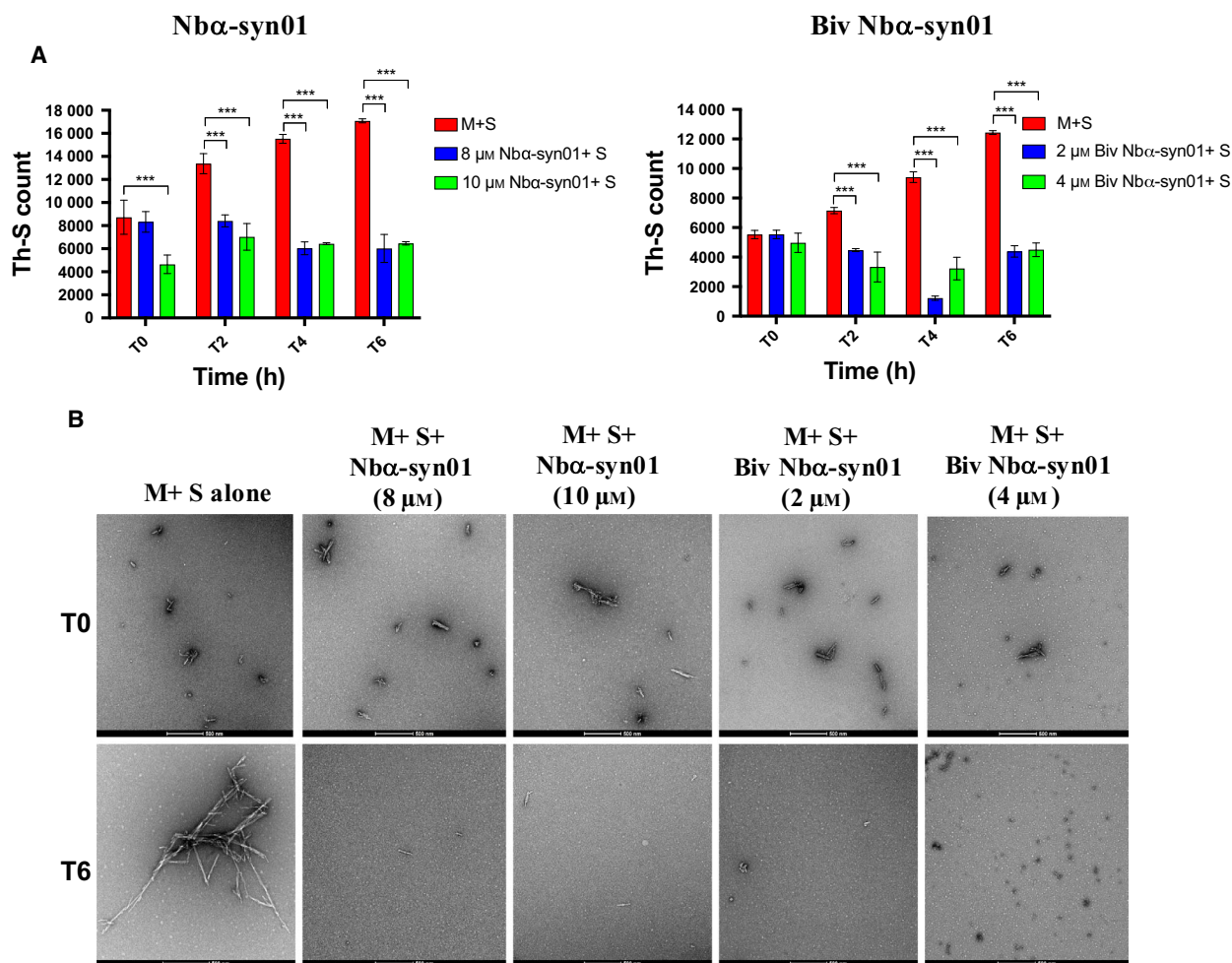


Fig. 5. (A) Th-S counts at different time points from the *in-vitro* seeding assay in presence of Nb α -syn01 and Biv Nb α -syn01 at different monomer concentration. Bar graph shows the mean and standard deviation (SD) of chemiluminescence signal (RLU·s⁻¹) obtained from duplicate values. Statistical analysis was performed using 2-way ANOVA with Tukey's multiple comparison test (*** P < 0.001; ** P < 0.01; * P < 0.05). (B) EM results from *in-vitro* seeding assay with monomers and seeds in presence of Nb α -syn01 and Biv Nb α -syn01 at different monomer concentrations at different time points as denoted. 'M' is monomeric form α -syn and 'S' is α -Syn seeds. Scale bars = 500 nm.

We selected the **5F10** (human CD38 in complex with nanobody MU551) for a template based on the highest global model quality estimation (GMQE) score of 0.69; quality estimation which combines properties from the target-template alignment. The modelled Nb α -syn01 structure exhibits the classical 9-stranded- β sandwich fold, a typical fold of the variable domains of an immunoglobulin, similar to its template and other nanobody structures (Fig. 8A). Structural comparison between modelled Nb α -syn01 and Nanobody MU551 (PDBID: **5F10**) showed that the structures are very similar, with an r.m.s.d. value of 0.11 Å. Similarly, comparison between modelled Nb α -syn01 and camelid-derived antibody fragment Nb7 (PDBID: **5LHN**) highlights the conservation of immunoglobulin fold with an r.m.s.d. value of 0.59 Å (Fig. 8B).

Structural superimposition of these structures also defines the variation in the complementarity-determining region 3 (CDR3). Although the conformations of the CDR1 and CDR2 regions are maintained, large differences can be observed on the CDR3 regions, notably in terms of size and conformation.

Molecular docking of modelled Nb α -syn01 and α -synuclein peptide (43–56) was performed by HPEP-DOCK docking server [37,38]. HPEPDOCK performs protein–peptide docking through a hierarchical algorithm and instead of running lengthy simulations; it considers the peptide flexibility through an ensemble of peptide conformations generated [38]. The peptide binds in long groove adjacent to CDR3 of Nb α -syn01 (Fig. 8C,D). The detailed interaction analysis shows a significant number of interactions with the important

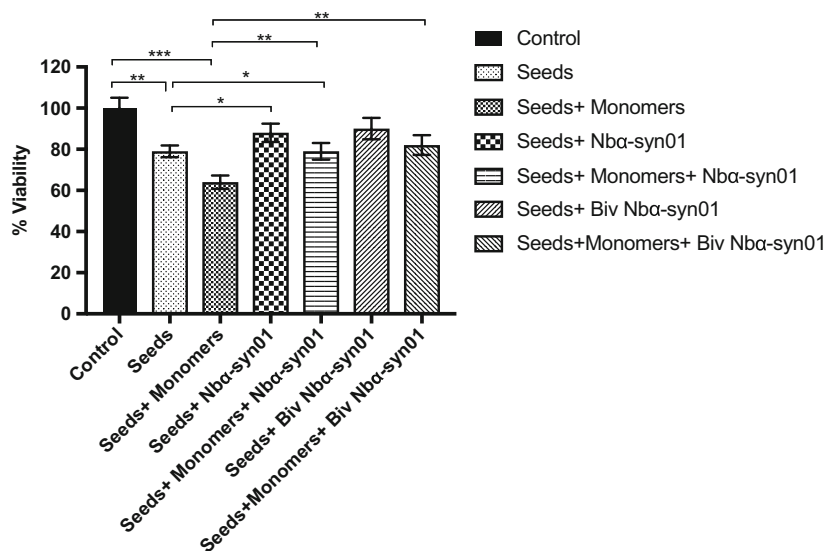


Fig. 6. Nb α -syn01 and BivNb α -syn01 inhibit the toxicity caused by α -syn seeds in SH-SY5Y cell model of PD. SH-SY5Y cell viability was evaluated using MTT assay. α -Syn seeds (2 μ M) were incubated with (2 μ M) Nb α -syn01 or (2 μ M) BivNb α -syn01 and added to cells in two separate sets. After 1 h of incubation, 10 μ M α -syn monomers were then added in Opti-MEM in one set and in another set Opti-MEM was added, incubation was further carried out for 48 h, prior to MTT addition. Newly formed formazan crystals were dissolved using solubilization buffer and the absorbance was measured and percentage of the viable cells was plotted (average of 3 wells \pm standard deviation). The results are expressed as percentages of the average of the control (untreated cells). Statistical analysis was performed using one-way ANOVA with Dunnet's multiple comparison test (** P < 0.001; ** P < 0.01; * P < 0.05).

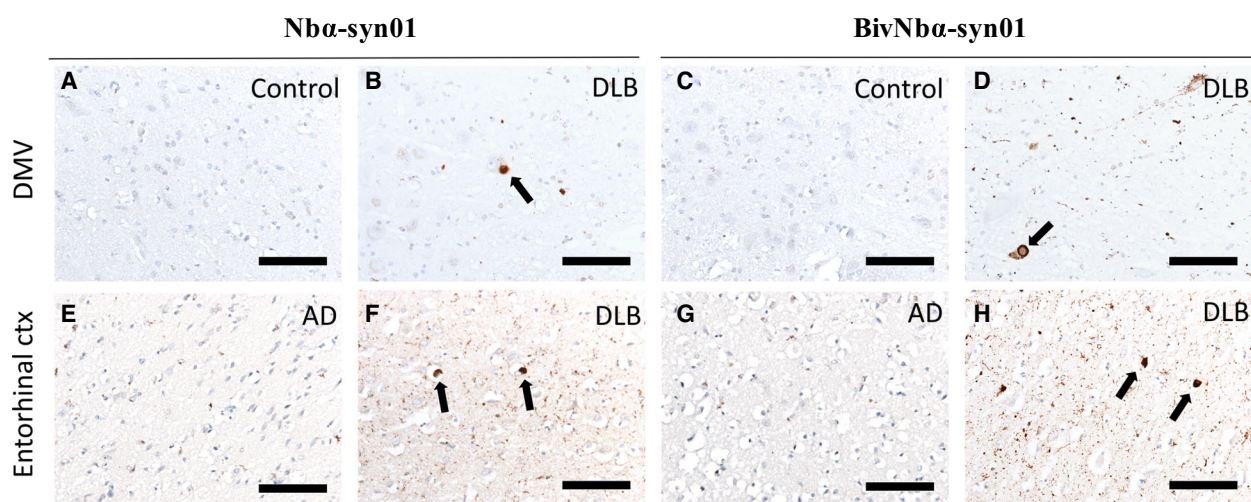


Fig. 7. Immunohistochemical staining of nanobodies in *post-mortem* brain tissue. Representative images demonstrating staining in the dorsal motor nucleus of the vagal nerve (DMV; A–D) or entorhinal cortex (E–H). Cases with Lewy body disease (B, D, F, H) are compared to control cases in the DMV (A, C) or disease-control Alzheimer's disease (AD) cases in the entorhinal cortex (E, G). Scale bars = 100 μ m.

residues of the Nb α -syn01 involving electrostatic based interaction of Arg 98, Arg100 and Gln109 from the Nb α -syn01 and T44, K45 and T54 from the α -syn (Fig. 8D). Overall, the peptide fit well into the deep cavity of the Nb α -syn01 binding region and interacts throughout the peptide length to the nanobody.

Further, to understand the interaction of nanobody to α -synuclein fibril, molecular docking of modelled Nb α -syn01 and α -synuclein fibril was performed by HDOCK docking server [39,40]. The modelled Nb α -syn01 docks at the interface of two protofilaments (Fig. 8E–G). α -Syn subunits in each protofilament stack along the fibril

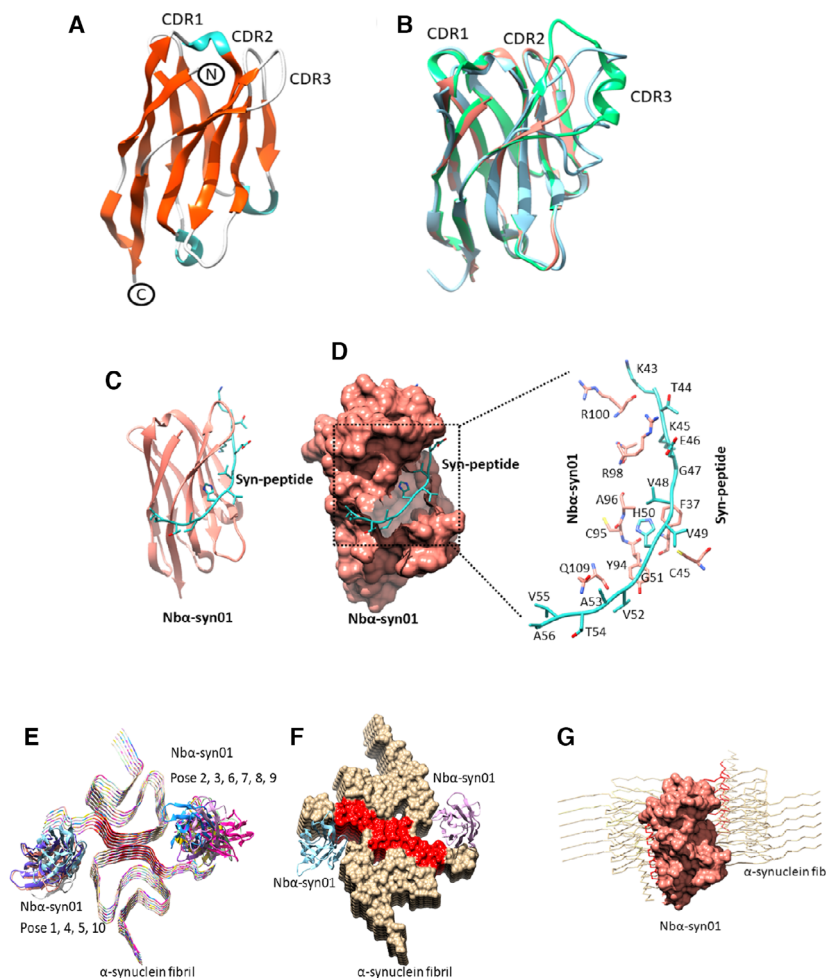


Fig. 8. (A, B) Overall structure of modelled Nb α -syn01. (A) Cartoon representation of modelled Nb α -syn01. Protein is coloured based on secondary structures; helix as green, β -strand as red and loop as grey. The complementarity-determining regions (CDRs), N and C-terminals are highlighted. (B) Structural superimposition of modelled Nb α -syn01 (salmon) with nanobody MU551 (PDBID: 5F10, green) and camelid-derived antibody fragment Nb7 (PDBID: 5LHN, blue). The three structures are highly similar in the overall fold with maximum variation in the CDR3 region. (C, D) Figure docking peptide: Potential binding of modelled Nb α -syn01 to α -synuclein peptide. Molecular docking of modelled Nb α -syn01 onto α -synuclein peptide represented as cartoon (C) and surface (D). Boxed zoom-in view shows binding pocket and residues involved in mediated the interaction. (E–G) Figure docking Nb α -syn01-fibril: Molecular docking of modelled Nb α -syn01 to α -synuclein fibril (PDBID: 6A6B) represented as cartoon (E) and surface (F). α -synuclein peptide regions are highlighted in red and are in proximity of Nb α -syn01. The Nb in (G) is presented in same orientation as '8D' with α -synuclein fibril as sticks and the peptide regions are highlighted in red.

axis with a helical twist and protofilaments intertwined along symmetrical screw axis [41]. All the poses interact with the fibril at the protofilament interface, where α -syn peptide region is located, which is considered as the most stable region of the fibril [41].

Discussion

Nb α -syn01 recognizes a key region in the N-terminal of α -syn

We describe here the development and characterization of a nanobody Nb α -syn01 and its bivalent format targeting α -syn. Epitope mapping showed that, unlike previously discovered Nbs that recognizes C-terminal region, Nb α -syn01 recognizes the N-terminal region of α -syn corresponding to amino acids 43–56 of α -syn. This as part of a region named PreNAC is known to aggregate onto amyloid-like fibrils in isolation [30,34]. Interestingly, this N-terminal region of α -syn has been prone to many autosomal dominant mutations that

cause familial early onset PD [5–10]. This region is also critical for aggregation *in vitro* and *in vivo*, and have an important role in mediating the membrane fusion of α -syn [29,42,43]. Taking account of all these considerations, the region recognized by our Nb is a key target to prevent α -syn aggregation. Importantly, Nb α -syn01 has high specificity to α -syn and did not bind to β or γ -syn unlike other N-terminal α -syn targeted antibodies that bind equally well with both β - or γ -syn [44,45]. C-terminal antibody binding can be affected by various post-translational modifications commonly found in the C-terminal region which is not present in the N-terminal binding antibodies such as Nb α -syn01 and BivNb α -syn01.

The engineered nanobodies recognize the monomeric, oligomeric and fibrillar form of α -syn with different affinities

While the immunization of the camel was done by the monomeric form of α -syn, the ITC and slot blot

showed unexpected results where Nb α -syn01 and its bivalent format favour the fibrillar form with higher affinity than the monomeric form. This might potentially be due to more than one Nb binding to the fibrillar entity. The engineered bivalent format showed an increased binding to aggregated forms due to higher avidity by the combination of two paratopes in the same entity. Both Nb formats additionally showed preference to α -syn HNE oligomers compared to dopamine oligomers. This preference of Nbs for particular aggregates is due to the differences in their respective unique structures. As a proof of concept, the binding of our Nbs to these aggregate forms may help in the maintenance of physiological homeostasis of their target by clearing specifically the misfolded proteins. Further characterization and improvement of the affinity and specificity are needed to have higher activity. The CD analysis of the complex formed between Nb formats and α -syn fibrils does not show a detectable perturbation in the structure after Nb binding. Previously, it has been reported that NbSyn87 and NbSyn2 were able to destabilize the structure of high-FRET oligomers and convert more toxic to less toxic oligomeric species of α -syn [28]. This may be due to their capability to access this specific epitope in fibrillar form because of their small size which causes a destabilization of the interactions of fibrils molecule.

The molecular docking of the Nb α -syn01-peptide shows that the peptide binds to the long groove of the Nb α -syn01 adjacent to CDR3 due to electrostatic-based interactions. However, this peptide forms a tight stack in the fibrils and is not completely exposed to the Nb in the Nb α -syn01-protofilaments model. According to our model, even though many Nb molecules can interact with the fibril, the peptide 43–56 that is part of the core structure and is near to the binding groove of nanobody, may not be fully involved in nanobody fibril interaction. It should be noted that the model for fibril-nanobody interaction is less reliable due to the complex multimeric nature of fibrils. We further analysed the same interactions using AlphaFold [46] resulting in unrealistic models. Further experiments involving crystallography of the Nb α -syn01-peptide complex along with affinity measurement of different mutated Nb α -syn01 with the monomeric and fibril forms of α -syn can give more insight into the mechanism of action.

Nb α -syn01 and BivNb α -syn01 inhibit *in-vitro* seeded aggregation and toxicity of α -syn

Nb α -syn01 and its bivalent formats were not only able to inhibit α -syn-seeded aggregation *in vitro* but also

reduced α -syn-seeded aggregation and toxicity in cells. As Nbs co-incubated with α -syn seeds reduced toxicity without concomitant application of monomers, this may indicate that Nbs might block the seeding for the endogenous α -syn monomers or reduce internalization of seeds and their related seeded aggregation of α -syn. The potential of the nanobody as passive immunotherapy is encouraging taking into account previous work utilizing antibodies targeting α -syn that has shown promising results in numerous *in vitro* and *in vivo* models as well as several clinical trials to reduce α -syn pathology and associated deficits [47–51]. However, the main obstacle for developing an antibody-based therapy that targets CNS is the blood-brain barrier (BBB) which has been shown to restrict the permeability of peripherally administered antibody to as low as 0.1% of antibody in blood gain CNS [52], necessitating high and frequent doses of antibody administration. Therefore, the use of the nanobodies can offer multiple advantages compared to conventional antibodies owing to their high affinity, specificity, stability and small size. Moreover, it was demonstrated that some Nbs with basic isoelectric point can cross the BBB after peripheral injection [53,54]. However, further work is required to demonstrate the physiological effects of aggregation inhibition by Nbs described here in other *in vivo* animal models of PD. The detection of Lewy bodies in post-mortem human PD brain tissue demonstrates that our Nbs have the potential as a diagnostic tool in synucleinopathies. Taken together, these findings suggest that our Nbs could be useful for development as therapeutic or diagnostic tools for PD.

Conclusion

We report the generation of a nanobody, Nb α -syn01, and its engineered bivalent form, BivNb α -syn01, that targets an important N-terminal region of α -syn. They recognize α -syn fibrils with higher affinities and inhibit aggregation and rescue cellular toxicity *in vitro*. These findings demonstrate that nanobodies could be a potential immunotherapeutic candidate in neurodegenerative diseases and highlight the potential of these particular nanobodies for PD and related synucleinopathies.

Materials and methods

Library construction

The study was approved by the Institutional Animal Care and Use Committee from the Ministry of Public Health in Qatar. A 3-year-old healthy male camel was weekly

immunized ten times subcutaneously with α -syn monomers (1 mg per camel) emulsified in Freund's complete adjuvant followed by booster immunization in incomplete adjuvant. The antibody titre was checked by ELISA and booster immunization was continued until a high antibody titre was obtained. To construct the VHH library, we followed the protocol previously described [55]. Briefly, from the immunized camel, we extracted total RNA from lymphocytes of 100 mL peripheral blood, which was used in the subsequent step to synthesize the corresponding cDNA using SuperScript™ II Reverse Transcriptase. Thereafter, gene fragments encoded the variable domain until the CH2 domains were amplified with specific primers CALL001 (5'-GTCCTGGCTCTCTTCTACAAGG-3') and CALL002 (5'-GGTACGTGCTGTTGAACTGTTCC-3'). The 700 bp fragment (VHH-CH2 without CH1 exon and corresponding to heavy-chain antibodies) was separated from the 900 bp fragment (VH-CH1-CH2 exons, derived from heavy chain of dromedary classical antibodies) and eluted from an agarose gel. VHH genes were amplified by one additional PCR with nested primers annealing at the extremity of the framework-1 and framework-4 (VHH-BACK-SAPI (5'-CTTGGCTCTTCTGTGCAG CTG CAG GAG TCT GGR GGA GG-3') and Primers VHH-FORWARD-SAPI (5'-TGA TGC TCT TCC GCT GAG GAG ACG GTG ACCTGGGT-3') regions. The final PCR fragments were ligated into the phagemid vector pMECS-GG using Golden gate cloning method by the restriction sites SapI [55]. Ligated material was transformed in *E. coli* electrocompetent cells (TG1) and plated on Petri dishes containing LB-agar with 100 $\mu\text{g}\cdot\text{mL}^{-1}$ ampicillin. The colonies were scraped from the plates, washed and stored at -80°C in LB medium with glycerol (25% final concentration) until further use.

Selection of α -synuclein specific nanobody

Synuclein-specific nanobodies were selected by four consecutive rounds of *in vitro* phage display selection on a well plate coated with 10 μg antigen per well. Specific phage particles were eluted with 100 mM triethylamine (pH 10.0). The eluted particles were used to infect exponentially growing *E. coli* TG1 cells. Enrichments of specific phage particles were assessed by comparing phage particle titres eluted from coated wells versus wells without antigen. After four rounds of panning, individual colonies were picked and cultured in Terrific Broth [56]. The periplasmic extract was tested by ELISA for the presence of molecules recognizing the antigen. Positive clones were sequenced by the Sanger method.

Expression and purification of nanobodies

The plasmid containing the nanobody gene of the positive clone in ELISA was transformed into *E. coli* WK6 competent cells. The clone was grown in Terrific Broth [56]

supplemented with ampicillin, until the absorbance at 600 nm reached 0.9. Nanobody expression was then induced with 1 mM isopropyl dthiogalactopyranoside for 16 h at 28°C . After pelleting cells, the periplasmic proteins were extracted by osmotic shock [57]. This periplasmic extract was loaded on a HisTrap HP 5 mL (Amersham Bioscience, Uppsala, Sweden) column in FPLC. After washing, the histidine tagged proteins were eluted with 250 mM imidazole. The eluted fraction was dialyzed against PBS and the purity was checked by SDS/PAGE and the final yield was determined by BCA quantification kit (Thermo Scientific™, Rockford, IL, USA).

Bivalent nanobody construction and purification

The genes encoding the Nb were amplified with primers DS40, 5'-GCC TGA TTC CTG CAG TTG TAC GTC ACT TGC CGG TGG TGT GGA TGG TGA TGG TGT GGG AGG TGT AGA TGG GCT TGA GGA GAC GGT GAC CTG GGT CCC-3', DS39 5'-GCG GCC CAG CCG GCC ATG GCC GAT GTG CAG CTA CAG GAG TCT GGG GGA GGC-3', to introduce the NcoI extremity of the VHH and the human IgA hinge (Ser Pro Ser Thr Pro Pro Thr Pro Ser Pro Ser Thr Pro Pro Ala Ser) and PstI restriction enzyme site at the 3' extremities of the amplified fragment of the VHH. The PCR-amplified product was then purified with Qiaquick PCR purification kit (Qiagen, Valencia, CA, USA) and digested overnight with NcoI/PstI. The digested fragment was purified again using the same PCR purification protocol. Meanwhile, the recombinant pMECS-GG plasmid containing the Nb gene was digested for several hours with NcoI/PstI enzymes. Finally, the recombinant plasmid and the PCR fragment were mixed and ligated with T4 DNA ligase. The ligated product was used to transform *E. coli* WK6 competent cells. Clones were screened by PCR using the universal forward MP57 and reverse GIII sequencing primers for the presence of the bivalent construct. Clones with amplification product of 1000 bp were sequenced to ensure the sequence and the absence of mutations. After expression, the encoded protein was tested for binding to α -syn and compared to monovalent nanobody by slot blot. To obtain larger amounts of the tandemly linked bivalent Nb construct, the protocols of purification were followed with the same conditions of the monovalent Nbs (see above).

Pepscan for epitope mapping

Epitope mapping was carried out as described previously [15]. Briefly, fourteen amino acid long peptides, with seven amino acid overlap, covering the entire sequence of α -syn (Fig. 1C) or recombinant α -syn, were coated onto a 384-well black MaxiSorp ELISA plate (Nunc, Roskilde, Denmark). The wells were dried overnight at 37°C and then blocked with 2.25% gelatin in PBST (PBS containing 0.05% Tween 20) for 1 h at room temperature (RT). After washing with PBST, 50 μL per well ($1\ \mu\text{g}\cdot\text{mL}^{-1}$) of our

Nb α -syn01 was added to the plate and incubated for 1 h at RT followed by washing and adding anti-His antibody (Abcam, Cambridge, UK) at 1/1000 dilution. The plate was washed and incubated with HRP-conjugated goat anti-mouse IgG secondary antibody for 1 h at RT. The bound HRP was detected by adding 50 μ L per well of the substrate (Super Signal ELISA Femto Maximum Sensitivity Substrate; Pierce Biotechnology, Rockford, IL, USA) and the chemiluminescence in relative light units measured with a Victor X3 2030 multi-label plate reader (Perkin Elmer, Hambourg, Germany). For the preabsorption experiment, Nb α -syn01 was mixed with either 500, 250 or 125 μ M of the peptides for 2 h at RT and then added to a 384 well plate coated with recombinant α -syn. The plate was washed and incubated with HRP-conjugated secondary antibody for 1 h at RT and developed as mentioned before.

Preparation of α -syn fibrils, seeds, oligomers and monomers

Full-length recombinant α -syn was expressed and purification was done as previously described [14]. The various forms of α -syn were generated as previously shown [58]. In summary, to make α -syn fibrils, α -syn monomers (50 μ M) were aged in PBS for 5 days at 37 °C with shaking continuously at 800 r.p.m. α -Syn fibrils generation was detected by Th-S fluorescence assay, and α -syn seeds were formed by fragmentation of mature α -syn fibrils via sonication. To make fresh monomers, α -syn was filtered through a 100 kDa molecular weight cut-off (MWCO) filter to remove higher size protein aggregates.

HNE-/ONE- α -syn oligomers were prepared using the protocol previously reported [59]. For the generation of HNE-/ONE- α -syn oligomers, α -syn was first dialysed against 50 mM disodium hydrogen phosphate, pH 8.5 followed by filtration using 100-kDa MWCO micron spin filter (Merck Millipore, Watford, UK) to get rid of high molecular weight aggregates. HNE was then added to α -syn monomers (140 μ M) to a final molar ratio of 30 : 1 (HNE : α -syn) followed by incubation of the samples at 37 °C for 18 h without shaking. The protein samples were centrifuged at 16 900 *g* for 5 min and the oligomeric species generated were separated by size exclusion chromatography on a Superdex 200 gel filtration column (GE Healthcare, Uppsala, Sweden) equilibrated with 20 mM Tris pH 7.4, 0.15 M NaCl buffer. The eluted peak fractions corresponding to the oligomeric fraction was pooled and quantified using BCA protein assay kit after solubilizing the oligomers in equal volume on 6 M GnHCl.

Affinity measurement by isothermal titration calorimetry

The binding of nanobody to α -synuclein was carried out by ITC using a MicroCal Auto-iTC200 microcalorimeter (Malvern Panalytical company, Malvern, PA, USA) at 25 °C. The

nanobody (120 μ L of 300 μ M of Nb α -syn01, 134 μ M of biv Nb α -syn01, syringe) was titrated into the sample cell, containing α -synuclein (400 μ L of 10 μ M of monomeric alpha syn or 40 μ M of Fibrils), sequentially by injecting a 2 μ L aliquot at each titration point with a time interval of 120 s. Total of 20 injections of the nanobody was mixed into α -synuclein cell with a stirring speed of 750 r.p.m. The first initial small injection was used to minimize the impact of equilibration artefacts and was disregarded during the evaluation of the data. As a control experiment, buffer solution was used in a sample cell with the same concentration of nanobody in the syringe. The heats of mixing and dilution of the control experiment were subtracted from the heat of binding per injection. To determine the equilibrium dissociation constant (K_d) and the enthalpic change (ΔH) associated with binding, the ITC isotherms were iteratively fit to a one-site binding model by non-linear least squares regression analysis using the MicroCal PEAQ-ITC analysis software (Malvern Panalytical company).

Blotting using vacuum filtration assay

The blotting system using the vacuum filtration method (Fisher Scientific, Rockford, IL, USA) was assembled with a pre-wet 0.2 μ m nitrocellulose membrane using the manufacturer's protocol. Specified quantities of antigen were prepared in 50 μ L PBS and applied to each slot. Following this, the wells were washed with 1000 μ L PBS and the membrane was then air-dried for 45 min. The dried membrane was blocked with 5% skimmed milk in 0.05% PBST for 1 h at RT. After blocking, the membranes were incubated overnight in generated Nbs or control antibodies diluted in 0.05% PBST at the following specified concentrations: Nb α -syn01 and BivNb α -syn01 (250 ng·mL⁻¹); 82E1 (Ms mAb for Abeta, IBL America, Minneapolis, MN, USA, 50 ng·mL⁻¹), 5E2 (Ms mAb for Tau, kindly provided by D. Walsh, Harvard Medical School, 50 ng·mL⁻¹), Anti-ABri (Rabbit anti-ABri antiserum, kindly provided by D. Walsh, Harvard Medical School, 1/3000); FL140 (Rb pAb for α -syn, from Santa Cruz Biotech, Dallas, TX, USA, 1 : 5000); F11 (Ms mAb for α/β syn, Santa Cruz Biotech (discontinued), 1 : 2000) and E20 (Gt pAb for Y-syn, Santa Cruz Biotech, 1 : 2000). For blots probed with Nbs, after overnight incubation with respective Nb, an additional Anti His (Ms mAb from Abcam, 1 : 2000) was applied for 2 h at RT. Following primary Ab incubation, blots were washed three times and incubated in respective HRP conjugated secondary Ab (1 : 20k for mAbs and 1 : 100k for pAbs) for 1 h at RT and detected using west pico (mAb) or west femto (for pAbs) chemiluminescent substrate and imaged using BioRad Imaging System (Feldkirchen, Germany).

Circular dichroism spectroscopy measurement

The perturbation of the secondary structure was checked by CD. CD spectra were obtained using a Chirascan CD spectrometer (Applied Photophysics, Leatherhead, Surrey,

UK) equipped with a water bath to control the temperature at 25 °C. The temperature for the experiments was controlled with a Peltier temperature control unit (Quantum northwest). α -Syn monomeric, pure fibrils, Nb α -syn01 and Biv Nb α -syn01 alone or in complex were diluted at 5 μ M in 300 μ L of PBS and the measurement was performed between 200 and 250 nm. Cells with path lengths of 1 mm were used and five scans were averaged to obtain each spectrum and final spectra were obtained by subtracting them from buffer spectra. The secondary structure modification was checked by subtraction of the signal of the complex to those of the Nb and its antigen alone.

MTT assay

To perform MTT assay, we plated SH-SY5Y cells in a 96-well MaxiSorp plate (Nunc), 15 000 cells (200 μ L per well) and incubated for 24 h in a CO₂ incubator at 37 °C. α -Syn pure seeds (2 μ M) were mixed with either Nb α -syn01 (0.25 μ M) or BivNb α -syn01 (0.25 μ M) using 100 μ L Opti-MEM for 30 min at 37 °C with 300 r.p.m. shaking. The media was removed and 100 μ L Opti-MEM containing seeds and antibodies was added to the cells. α -Syn monomers (10 μ M) were added in another 100 μ L Opti-MEM to the cells after 1 h and incubated for a further 48 h. Wells containing Opti-MEM were control wells and had no treatment, and blank wells consisted of no cells. The 96-well plate was further incubated at 37 °C for 4.5 h after the addition of 20 μ L of 6 mg·mL⁻¹ MTT to each well. 100 μ L per well of 15% (w/v) SDS, 50% (v/v) *N,N*-dimethylformamide, pH 4.7, was added after the removal of medium-MTT solution and the plate was again incubated overnight at 37 °C. The resultant absorbance was detected using Nano Quant instrument by TECAN (Männedorf, Switzerland) at 590 nm wavelength.

In-vitro seeded aggregation assay

α -Syn seeds (1 μ M) in PBS pH 7.4 were incubated alone or in combination with Nb α -syn01 (8 and 10 μ M) or BivNb α -syn01 (2 and 4 μ M), in sealed 1.5 mL sterile polypropylene tubes for 1 h at 37 °C with continuous shaking at 300 r.p.m. (total volume = 100 μ L). α -Syn monomers (25 μ M) were then added in PBS to a total volume of 500 μ L, and the reaction mixture was further incubated at 37 °C with continuous shaking at 800 r.p.m. Protein sample aliquots were taken out at 0, 2, 4 and 6 h intervals and immediately flash-frozen in liquid nitrogen. α -Syn aggregation was determined using Th-S fluorescence assay. Each sample (10 μ L) was mixed with Th-S reagent (40 μ L–25 μ M) in PBS. Resultant fluorescence was detected in a 384-well, non-treated, black microwell plate (Nunc) with a Perkin Elmer EnVision Multimode Plate Reader using 450 and 486 nm excitation and emission wavelengths respectively.

Transmission electron microscopy

Protein samples for electron microscopy images were prepared by depositing them on Formvar-coated 400 mesh copper grids followed by fixing briefly with 0.5% glutaraldehyde and negatively staining with 2% uranyl acetate. Images were acquired using FEI Talos 200 C electron microscope (ThermoFisher Scientific, Rockford, IL, USA).

Immunohistochemistry

Post-mortem brain tissue from DMV of one control and one DLB case, and entorhinal cortex of one AD case and one DLB case, was obtained from Newcastle Brain Tissue Resource, Newcastle University, UK and stained with Nb_M_01 or BivNb_M01. After dewaxing and epitope unmasking using boiling citrate pH 6 and formic acid, tissue sections were incubated with the two Nb formats for 1 h at room temperature (Nb_M_01, 1 μ g·mL⁻¹; BivNb_M01, 250 ng·mL⁻¹). To determine Nb binding, we used an antibody against the polyhistidine tag (ab18184, Abcam; 0.5 mg·mL⁻¹) conjugated to Nbs for 1 h at room temperature. Primary antibody binding was then visualized with Menarini MenaPath kits (Menarini Diagnostics, Wincersh, UK) according to the manufacturer's instructions, and counterstained with haematoxylin. Donors or next of kin provided informed consent to donate tissue and all procedures were approved by Newcastle Brain Tissue Resource Ethics Committee and the local UK National Health Service Research Ethics Committee. Sections were visualized and images obtained using a Nikon Eclipse 90i microscope coupled to a computer with NIS Elements software (Nikon, Tokyo, Japan).

Protein modelling and docking

In absence of experimentally determined structure of the Nb α -syn01, structure based homology modelling was employed. We used SWISS-MODEL to generate the 3D structure of Nb α -syn01 [36]. Template search matching Nb α -syn01 protein sequence with BLAST [60] and HHBLITS [61] was performed against the SWISS-MODEL template library. Nanobody MU551 complexed with human CD38 (PDBID: 5F1O) was selected based on the protein sequence coverage and sequence identity (sequence identity of 64.84%). The quality of the predicted model was examined by MOLPROBITY [62], a structure validation server, which revealed the results in terms of phi, psi and C β deviations by generating a Ramachandran plot for the resulted model. The model generated is of good quality with 97.39% of the residues in Ramachandran favoured region. The quaternary structure annotation of the template is used to model the Nb α -syn01 in its oligomeric form. The quaternary structure quality estimate (QSQE) method was used which combines

interface conservation, structural clustering, and other template features to provide a quaternary structure [63].

We performed protein peptide (Nb α -syn01–synuclein peptide) docking using HPEPDOCK docking server [37,38]. We use modelled nanobody structure as a receptor and provided the peptide sequence in fasta format as an input. We performed the docking with default parameters and 10 predicted conformers (poses) were further analysed. Similarly, we also performed molecular docking of Nb α -syn01 with α -synuclein fibril structure (PDBID: 6A6B, comprising amino acids 37–99) using HDOCK docking server [39,40]. Due to the large size of fibril, it was used as a receptor and modelled Nb α -syn01 as ligand. We performed the docking with default parameters and 10 predicted conformers (poses) were further analysed. All structural analysis, figures with structure representations and superimposition were produced using the program UCSF CHIMERA [64].

Acknowledgements

Prof El-Agnaf's laboratory is funded by Qatar Biomedical Research Institute. The authors would like to express their sincere thanks to imaging and characterization core laboratory at Qatar Environmental and Energy Research Institute specially Janarthanan Ponraj and Dr Said Mansour. The authors also extend their thanks to the camel animal facility 'Al-Halal Lilhrajat Wllmdhadat Llmwashy', especially to Mr. Mohd Ali Al-Marri.

Conflict of interest

The authors declare no conflict of interest.

Author contributions

IH, NNV, NKM and OMAE-A designed the project and contributed the research questions. IH, OMAE-A, NNV, IPS, VG, SSG, MME, HBA and DE wrote and edited the manuscript, and presented results in visual forms. OMAE-A supervised the project and contributed to the project design. PRK and ZI handled modelling and docking experiment. DKA, TV, IH and NNK handled immunization of camel and blood collection. All the authors contributed to editing of the manuscript. No honorarium, grant or other form of payment was given to any of the authors to produce the manuscript.

Peer review

The peer review history for this article is available at <https://publons.com/publon/10.1111/febs.16376>.

Data availability statement

The authors confirm that the data supporting the findings of this study are available within the article.

References

- Baba M, Nakajo S, Tu PH, Tomita T, Nakaya K, Lee VM, et al. Aggregation of alpha-synuclein in Lewy bodies of sporadic Parkinson's disease and dementia with Lewy bodies. *Am J Pathol.* 1998;**152**:879–84.
- Newell KL, Boyer P, Gomez-Tortosa E, Hobbs W, Hedley-Whyte ET, Vonsattel JP, et al. Alpha-synuclein immunoreactivity is present in axonal swellings in neuroaxonal dystrophy and acute traumatic brain injury. *J Neuropathol Exp Neurol.* 1999;**58**:1263–8.
- Wakabayashi K, Yoshimoto M, Tsuji S, Takahashi H. Alpha-synuclein immunoreactivity in glial cytoplasmic inclusions in multiple system atrophy. *Neurosci Lett.* 1998;**249**:180–2.
- Arawaka S, Saito Y, Murayama S, Mori H. Lewy body in neurodegeneration with brain iron accumulation type 1 is immunoreactive for alpha-synuclein. *Neurology.* 1998;**51**:887–9.
- Krüger R, Kuhn W, Müller T, Woitalla D, Graeber M, Kösel S, et al. Ala30Pro mutation in the gene encoding alpha-synuclein in Parkinson's disease. *Nat Genet.* 1998;**18**:106–8.
- Chi Y-C, Armstrong GS, Jones DNM, Eisenmesser EZ, Liu C-W. Residue histidine 50 plays a key role in protecting α -synuclein from aggregation at physiological pH. *J Biol Chem.* 2014;**289**:15474–81.
- Rutherford NJ, Moore BD, Golde TE, Giasson BI. Divergent effects of the H50Q and G51D SNCA mutations on the aggregation of α -synuclein. *J Neurochem.* 2014;**131**:859–67.
- Polymeropoulos MH, Lavedan C, Leroy E, Ide SE, Dehejia A, Dutra A, et al. Mutation in the alpha-synuclein gene identified in families with Parkinson's disease. *Science.* 1997;**276**:2045–7.
- Fares M-B, Ait-Bouziad N, Dikiy I, Mbefo MK, Jovičić A, Kiely A, et al. The novel Parkinson's disease linked mutation G51D attenuates in vitro aggregation and membrane binding of α -synuclein, and enhances its secretion and nuclear localization in cells. *Hum Mol Genet.* 2014;**23**:4491–509.
- Zarranz JJ, Alegre J, Gómez-Esteban JC, Lezcano E, Ros R, Ampuero I, et al. The new mutation, E46K, of alpha-synuclein causes Parkinson and Lewy body dementia. *Ann Neurol.* 2004;**55**:164–73.
- Giasson BI, Murray IV, Trojanowski JQ, Lee VM. A hydrophobic stretch of 12 amino acid residues in the

- middle of alpha-synuclein is essential for filament assembly. *J Biol Chem.* 2001;**276**:2380–6.
- 12 Murray IVJ, Giasson BI, Quinn SM, Koppaka V, Axelsen PH, Ischiropoulos H, et al. Role of alpha-synuclein carboxy-terminus on fibril formation in vitro. *Biochemistry.* 2003;**42**:8530–40.
- 13 Fields CR, Bengoa-Vergniory N, Wade-Martins R. Targeting alpha-synuclein as a therapy for Parkinson's disease. *Front Mol Neurosci.* 2019;**12**:299.
- 14 Vaikath NN, Hmila I, Gupta V, Erskine D, Ingelsson M, El-Agnaf OMA. Antibodies against alpha-synuclein: tools and therapies. *J Neurochem.* 2019;**150**:612–25.
- 15 Vaikath NN, Majbour NK, Paleologou KE, Ardah MT, van Dam E, van de Berg WDJ, et al. Generation and characterization of novel conformation-specific monoclonal antibodies for α -synuclein pathology. *Neurobiol Dis.* 2015;**79**:81–99.
- 16 Masliah E, Rockenstein E, Mante M, Crews L, Spencer B, Adame A, et al. Passive immunization reduces behavioral and neuropathological deficits in an alpha-synuclein transgenic model of Lewy body disease. *PLoS One.* 2011;**6**:e19338.
- 17 Weihofen A, Liu Y, Arndt JW, Huy C, Quan C, Smith BA, et al. Development of an aggregate-selective, human-derived α -synuclein antibody BIIB054 that ameliorates disease phenotypes in Parkinson's disease models. *Neurobiol Dis.* 2019;**124**:276–88.
- 18 Emadi S, Liu R, Yuan B, Schulz P, McAllister C, Lyubchenko Y, et al. Inhibiting aggregation of alpha-synuclein with human single chain antibody fragments. *Biochemistry.* 2004;**43**:2871–8.
- 19 Emadi S, Kasturirangan S, Wang MS, Schulz P, Sierks MR. Detecting morphologically distinct oligomeric forms of α -synuclein. *J Biol Chem.* 2009;**284**:11048–58.
- 20 Emadi S, Barkhordarian H, Wang MS, Schulz P, Sierks MR. Isolation of a human single chain antibody fragment against oligomeric alpha-synuclein that inhibits aggregation and prevents alpha-synuclein-induced toxicity. *J Mol Biol.* 2007;**368**:1132–44.
- 21 Barkhordarian H, Emadi S, Schulz P, Sierks MR. Isolating recombinant antibodies against specific protein morphologies using atomic force microscopy and phage display technologies. *Protein Eng Des Sel.* 2006;**19**:497–502.
- 22 Lynch SM, Zhou C, Messer A. An scFv intrabody against the nonamyloid component of alpha-synuclein reduces intracellular aggregation and toxicity. *J Mol Biol.* 2008;**377**:136–47.
- 23 Hamers-Casterman C, Atarhouch T, Muyldermans S, Robinson G, Hamers C, Songa EB, et al. Naturally occurring antibodies devoid of light chains. *Nature.* 1993;**363**:446–8.
- 24 Center for Drug Evaluation and Research. FDA approved caplacizumab-yhdp. FDA; 2019.
- 25 De Genst EJ, Williams T, Wellens J, O'Day EM, Waudby CA, Meehan S, et al. Structure and properties of a complex of α -synuclein and a single-domain camelid antibody. *J Mol Biol.* 2010;**402**:326–43.
- 26 Williams T, El-Turk F, Buell AK, O'Day EM, Aprile FA, Esbjörner EK, et al. Nanobodies raised against monomeric α -synuclein distinguish between fibrils at different maturation stages. *J Mol Biol.* 2013;**425**:2397–411.
- 27 Butler DC, Joshi SN, Genst ED, Baghel AS, Dobson CM, Messer A. Bifunctional anti-non-amyloid component α -synuclein nanobodies are protective in situ. *PLoS One.* 2016;**11**:e0165964.
- 28 Iljina M, Hong L, Horrocks MH, Ludtmann MH, Choi ML, Hughes CD, et al. Nanobodies raised against monomeric α -synuclein inhibit fibril formation and destabilize toxic oligomeric species. *BMC Biol.* 2017;**15**:57.
- 29 van Ham TJ, Thijssen KL, Breitling R, Hofstra RMW, Plasterk RHA, Nollen EAA. *C. elegans* model identifies genetic modifiers of alpha-synuclein inclusion formation during aging. *PLoS Genet.* 2008;**4**:e1000027.
- 30 Rodriguez JA, Ivanova MI, Sawaya MR, Cascio D, Reyes F, Shi D, et al. Structure of the toxic core of α -synuclein from invisible crystals. *Nature.* 2015;**525**:486–90.
- 31 Wong YC, Krainc D. α -Synuclein toxicity in neurodegeneration: mechanism and therapeutic strategies. *Nat Med.* 2017;**23**:1–13.
- 32 Winner B, Jappelli R, Maji SK, Desplats PA, Boyer L, Aigner S, et al. In vivo demonstration that alpha-synuclein oligomers are toxic. *Proc Natl Acad Sci USA.* 2011;**108**:4194–9.
- 33 Mahul-Mellier A-L, Vercurysse F, Maco B, Ait-Bouziad N, De Roo M, Muller D, et al. Fibril growth and seeding capacity play key roles in α -synuclein-mediated apoptotic cell death. *Cell Death Differ.* 2015;**22**:2107–22.
- 34 El-Agnaf OM, Jakes R, Curran MD, Middleton D, Ingenito R, Bianchi E, et al. Aggregates from mutant and wild-type alpha-synuclein proteins and NAC peptide induce apoptotic cell death in human neuroblastoma cells by formation of beta-sheet and amyloid-like filaments. *FEBS Lett.* 1998;**440**:71–5.
- 35 Gupta V, Salim S, Hmila I, Vaikath NN, Sudhakaran IP, Ghanem SS, et al. Fibrillar form of α -synuclein-specific scFv antibody inhibits α -synuclein seeds induced aggregation and toxicity. *Sci Rep.* 2020;**10**:8137.
- 36 Waterhouse A, Bertoni M, Bienert S, Studer G, Tauriello G, Gumienny R, et al. SWISS-MODEL: homology modelling of protein structures and complexes. *Nucleic Acids Res.* 2018;**46**:W296–303.
- 37 Zhou P, Li B, Yan Y, Jin B, Wang L, Huang S-Y. Hierarchical flexible peptide docking by conformer generation and ensemble docking of peptides. *J Chem Inf Model.* 2018;**58**:1292–302.
- 38 Zhou P, Jin B, Li H, Huang S-Y. HPEPDOCK: a web server for blind peptide-protein docking based on a

- hierarchical algorithm. *Nucleic Acids Res.* 2018;**46**:W443–50.
- 39 Yan Y, Tao H, He J, Huang S-Y. The HDock server for integrated protein-protein docking. *Nat Protoc.* 2020;**15**:1829–52.
- 40 Yan Y, Zhang D, Zhou P, Li B, Huang S-Y. HDock: a web server for protein-protein and protein-DNA/RNA docking based on a hybrid strategy. *Nucleic Acids Res.* 2017;**45**:W365–73.
- 41 Li Y, Zhao C, Luo F, Liu Z, Gui X, Luo Z, et al. Amyloid fibril structure of α -synuclein determined by cryo-electron microscopy. *Cell Res.* 2018;**28**:897–903.
- 42 Fusco G, Pape T, Stephens AD, Mahou P, Costa AR, Kaminski CF, et al. Structural basis of synaptic vesicle assembly promoted by α -synuclein. *Nat Commun.* 2016;**7**:12563.
- 43 Lautenschläger J, Stephens AD, Fusco G, Ströhl F, Curry N, Zacharopoulou M, et al. C-terminal calcium binding of α -synuclein modulates synaptic vesicle interaction. *Nat Commun.* 2018;**9**:712.
- 44 Hashimoto M, Hsu LJ, Rockenstein E, Takenouchi T, Mallory M, Masliah E. α -Synuclein protects against oxidative stress via inactivation of the c-Jun N-terminal kinase stress-signaling pathway in neuronal cells. *J Biol Chem.* 2002;**277**:11465–72.
- 45 Uversky VN, Li J, Souillac P, Millett IS, Doniach S, Jakes R, et al. Biophysical properties of the synucleins and their propensities to fibrillate: inhibition of α -synuclein assembly by β - and γ -synucleins. *J Biol Chem.* 2002;**277**:11970–8.
- 46 Jumper J, Evans R, Pritzel A, Green T, Figurnov M, Ronneberger O, et al. Highly accurate protein structure prediction with AlphaFold. *Nature.* 2021;**596**:583–9.
- 47 George S, Brundin P. Immunotherapy in Parkinson's disease: micromanaging α -synuclein aggregation. *J Parkinsons Dis.* 2015;**5**:413–24.
- 48 Schneeberger A, Tierney L, Mandler M. Active immunization therapies for Parkinson's disease and multiple system atrophy. *Mov Disord.* 2016;**31**:214–24.
- 49 Valera E, Masliah E. Immunotherapy for neurodegenerative diseases: focus on α -synucleinopathies. *Pharmacol Ther.* 2013;**138**:311–22.
- 50 El-Agnaf O, Overk C, Rockenstein E, Mante M, Florio J, Adame A, et al. Differential effects of immunotherapy with antibodies targeting α -synuclein oligomers and fibrils in a transgenic model of synucleinopathy. *Neurobiol Dis.* 2017;**104**:85–96.
- 51 Volc D, Poewe W, Kutzelnigg A, Lührs P, Thun-Hohenstein C, Schneeberger A, et al. Safety and immunogenicity of the α -synuclein active immunotherapeutic PD01A in patients with Parkinson's disease: a randomised, single-blinded, phase 1 trial. *Lancet Neurol.* 2020;**19**:591–600.
- 52 Coloma MJ, Lee HJ, Kurihara A, Landaw EM, Boado RJ, Morrison SL, et al. Transport across the primate blood-brain barrier of a genetically engineered chimeric monoclonal antibody to the human insulin receptor. *Pharm Res.* 2000;**17**:266–74.
- 53 Li T, Bourgeois J-P, Celli S, Glacial F, Le Sourd A-M, Mecheri S, et al. Cell-penetrating anti-GFAP VHH and corresponding fluorescent fusion protein VHH-GFP spontaneously cross the blood-brain barrier and specifically recognize astrocytes: application to brain imaging. *FASEB J.* 2012;**26**:3969–79.
- 54 Li T, Vandesquille M, Koukoulis F, Duffeffant C, Youssef I, Lenormand P, et al. Camelid single-domain antibodies: a versatile tool for in vivo imaging of extracellular and intracellular brain targets. *J Control Release.* 2016;**243**:1–10.
- 55 Romão E, Poignavent V, Vincke C, Ritzenthaler C, Muyltermans S, Monsion B. Construction of high-quality camel immune antibody libraries. *Methods Mol Biol.* 2018;**1701**:169–87.
- 56 Sambrook JF, Russell D. Molecular cloning: a laboratory manual (3-volume set). New York, NY: Cold Spring Harbor Laboratory Press; 2001.
- 57 Skerra A, Pluckthun A. Assembly of a functional immunoglobulin Fv fragment in *Escherichia coli*. *Science.* 1988;**240**:1038–41.
- 58 Ardah MT, Paleologou KE, Lv G, Abul Khair SB, Kazim AS, Minhas ST, et al. Structure activity relationship of phenolic acid inhibitors of α -synuclein fibril formation and toxicity. *Front Aging Neurosci.* 2014;**6**:197.
- 59 Näsström T, Fagerqvist T, Barbu M, Karlsson M, Nikolajeff F, Kasrayan A, et al. The lipid peroxidation products 4-oxo-2-nonenal and 4-hydroxy-2-nonenal promote the formation of α -synuclein oligomers with distinct biochemical, morphological, and functional properties. *Free Radic Biol Med.* 2011;**50**:428–37.
- 60 Camacho C, Coulouris G, Avagyan V, Ma N, Papadopoulos J, Bealer K, et al. BLAST+: architecture and applications. *BMC Bioinformatics.* 2009;**10**:421.
- 61 Steinegger M, Meier M, Mirdita M, Vöhringer H, Haunsberger SJ, Söding J. HH-suite3 for fast remote homology detection and deep protein annotation. *BMC Bioinformatics.* 2019;**20**:473.
- 62 Chen VB, Arendall WB, Headd JJ, Keedy DA, Immormino RM, Kapral GJ, et al. MolProbity: all-atom structure validation for macromolecular crystallography. *Acta Crystallogr D Biol Crystallogr.* 2010;**66**:12–21.
- 63 Bertoni M, Kiefer F, Biasini M, Bordoli L, Schwede T. Modeling protein quaternary structure of homo- and hetero-oligomers beyond binary interactions by homology. *Sci Rep.* 2017;**7**:10480.
- 64 Pettersen EF, Goddard TD, Huang CC, Couch GS, Greenblatt DM, Meng EC, et al. UCSF Chimera – a visualization system for exploratory research and analysis. *J Comput Chem.* 2004;**25**:1605–12.